ISSN 1541-308X, Physics of Wave Phenomena, 2023, Vol. 31, No. 5, pp. 320–326. © Allerton Press, Inc., 2023.

OPTICAL SPECTROSCOPY

Passive Thermal Compensation of the Spectral Characteristic of the Integrated-Optical Demultiplexer

I. G. Likhachev[a], *, D. A. Guryev[a], V. I. Pustovoy[a], and K. E. Pevchikh[b]

[a] *Prokhorov General Physics Institute of the Russian Academy of Sciences, Moscow, 119991 Russia*

[b] *"Zelenograd Nanotechnology Center" Company, Zelenograd, Moscow, 124527 Russia*

**e-mail: iglikhachev@gmail.com*

Received April 28, 2023; revised April 28, 2023; accepted May 24, 2023

Abstract—The method of passive thermal compensation of the arrayed waveguide grating (AWG) demultiplexer based on a cut in the input planar waveguide and a controlled angle of rotation of a part of this waveguide is investigated. A possibility of performing this thermal compensation is shown, restrictions on the choice of the demultiplexer parameters to be observed for functioning of the demultiplexer are obtained, and relevant recommendations are given. A simple algebraic expression for the derivative of the compensation angle with respect to temperature is obtained, which is needed for development of the demultiplexer. In the given numerical example, this derivative is 3.5×10^{-5} rad/K.

Keywords: arrayed waveguide gratings, demultiplexer, athermal AWG, spectral characteristic, passive thermal compensation

DOI: 10.3103/S1541308X23050072

1. INTRODUCTION

In the past 30 years, arrayed waveguide gratings (AWGs) have been actively employed as multiplexers/demultiplexers in optical communication and telecommunication systems. With improvement of AWGs, devices on their basis have found application in many fields of science and technology, e.g., development of optical sensors [1, 2], Raman spectrometers [3], and multifrequency lasers [4]. In addition, AWGs are used in astronomy [5] and laser physics [6, 7].

The use of AWGs in real devices faces a number of serious problems. One of them is temperature drift of the central wavelength of the spectral characteristics, which can be no less than 0.1 nm/°C, unacceptably large for real applications. Therefore, development of AWGs with temperature drift compensation, so-called athermal AWGs, has become an in-demand research problem in the past years. Several approaches to performing thermal compensation have been proposed, such as active cooling [8, 9]; usage of materials with specially selected refractive indices, thermal expansion coefficient, and temperature dependence of the refractive index [10]; and passive thermal compensation methods [11–19].

One of the simplest and most effective ways of compensating the temperature drift is active cooling of an AWG [8, 9]. Devices of this kind require power supply, and, in addition, the cooling element considerably increases the size of the demultiplexer. Therefore, AWGs with passive thermal compensation capable of functioning independently arouse particular interest. Quite a lot of methods for passive thermal compensation have been developed, in which the temperature drift is decreased by using polymers with certain refractive indices as materials for waveguide arrays [10], by making polymer-filled grooves in the input planar waveguide [11, 12], by making a cut or a cascade of cuts in the waveguide array [13–15], and by making controlled cuts in the input/output planar waveguide [16–19]. These methods allow the central wavelength temperature drift to be decreased to 0.01 nm/°C, but these technical solutions are quite difficult to implement because of strict requirements on the precision of the AWG chip fabrication and on the circuit calculation.

Calculations of circuit designs for most athermal AWGs can be found in the literature. The method of thermal compensation using a controlled cut in the input planar waveguide is considered, to the best of our knowledge, in the patent [19], where several technical designs are proposed, but no method for calculation of their optical and thermal characteristics is given. In this work, a similar demultiplexer is analyzed, relations needed for its development are obtained, and recommendations and restrictions on the choice of parameters ensuring its functioning are given.

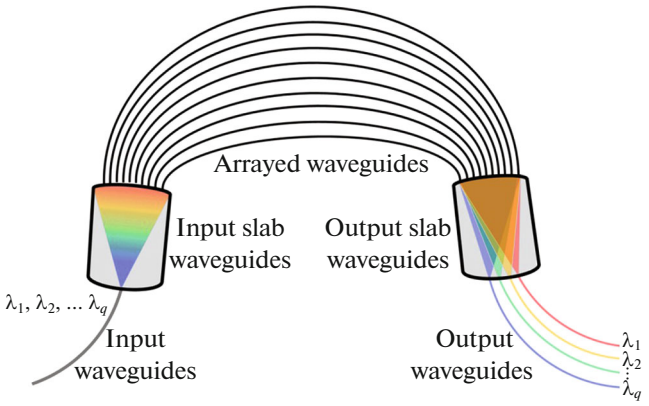

Fig. 1. (Color online) Structure of the AWG demultiplexer.

2. UNPERTURBED DEMULTIPLEXER

Let us first consider the initial demultiplexer, i.e., the device without a cut in its input planar waveguide (Fig. 1).

The optical path length of a wave propagating in the channel with number j ($j = -M, ..., 0, ..., M$; the total number of channels is $N = 2M + 1$) and entering the receiving waveguide with number q is defined by the relations

$$H_{jq}^{(0)} = n_{\text{pl}} R_{\text{in}} + n_{\text{ch}} L_j + n_{\text{pl}} R_{\text{ex}} f_{jq}, \tag{1}$$

$$L_j = L_0 + j\Delta L, \tag{2}$$

where L_j is the length of the jth channel, ΔL is the difference of the lengths of the neighboring channels, R_{in} and R_{ex} are the circle radii at the demultiplexer input and output (see Figs. 2 and 3), n_{pl} and n_{ch} are the refractive indices of the planar and channel waveguides, and the dimensionless factor f_{jq} is calculated by the formula

$$f_{jq} = 1 - \frac{1}{8}\beta_q^2 - \frac{1}{2}\beta_q \alpha_j, \tag{3}$$

where the meaning of the angles α_j and β_q is clear from Fig. 3. Since $\alpha_j = j\Delta\alpha$, where $\Delta\alpha$ is the step of variation of the angle α_j, formula (3) can be rewritten as

$$f_{jq} = f_{0q} - \frac{1}{2}\beta_q j\Delta\alpha, \tag{4}$$

where $f_{0q} = 1 - \frac{1}{8}\beta_q^2$. Now formula (1) is reduced to the form

$$H_{jq}^{(0)} = H_{0q}^{(0)} + (\Delta H)_q j, \tag{5}$$

where

$$H_{0q}^{(0)} = n_{\text{pl}}\left(R_{\text{in}} + R_{\text{ex}} f_{0q}\right) + n_{\text{ch}} L_0, \tag{6}$$

$$(\Delta H)_q \equiv n_{\text{ch}}\Delta L - \frac{1}{2} n_{\text{pl}} b_{\text{ex}} \beta_q, \tag{7}$$

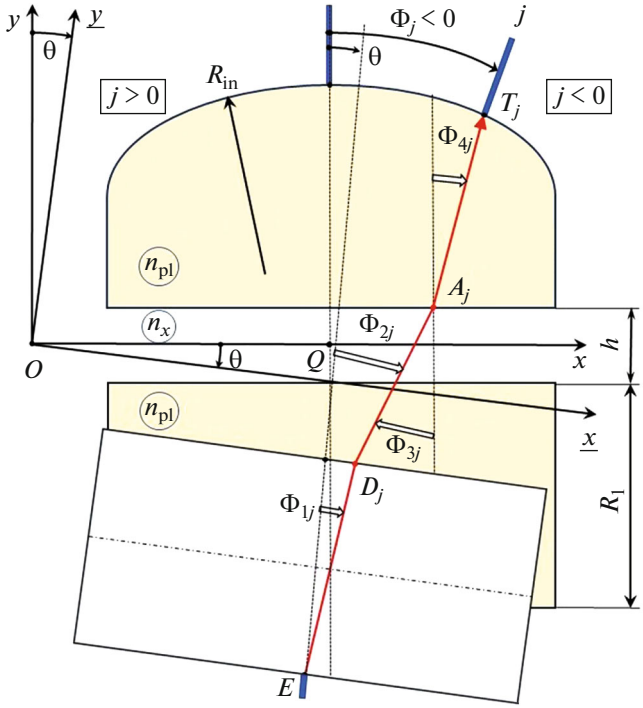

Fig. 2. (Color online) Input planar waveguide (Free Propagation Region, FPR) with a cut.

and the following relation is used (see Fig. 3):

$$R_{\text{ex}}\Delta\alpha = b_{\text{ex}}. \tag{8}$$

3. DEMULTIPLEXER WITH A CUT

Now we consider a demultiplexer (see Fig. 2) in which the input planar waveguide has a cut with width h and a part of the waveguide is rotated by an angle θ ($|\theta| \ll 1$). The cut is filled with a plastic dielectric with refractive index n_x. As a result, in (5) there appears perturbation δH_j

$$H_{jq} = H_{0q}^{(0)} + (\Delta H)_q j + \delta H_j. \tag{9}$$

In the Appendix, it is shown that calculation of δH_j leads to

$$\delta H_j = n_j h_j - n_{\text{pl}} h\cos\Phi_j + \frac{n_x^2}{n_j}\left[|h_j| - h_j\right], \tag{10}$$

where the following notation is introduced:

$$n_j \equiv \sqrt{n_x^2 - n_{\text{pl}}^2 \sin^2\Phi_j}, \tag{11}$$

$$h_j = h_j(\theta) \equiv h + (X_Q - R_1 \tan\Phi_j)\theta. \tag{12}$$

Here n_x is the refractive index of the medium filling the cut, and the meaning of distances X_Q and R_1 is clear from Fig. 2. Angles Φ_j are dictated by the unperturbed device and are calculated by the formula

$$\Phi_j = \frac{b_{\text{in}}}{R_{\text{in}}} j, \tag{13}$$

where b_{in} is the period of arrangement of the waveguide channels at the input.

Further we consider the region of parameters where the condition

$$h_j \geq 0 \tag{14}$$

is fulfilled.

This inequality will be verified below. In this region, the last term in (10) disappears, and we obtain

$$\delta H_j = h(n_j - n_{\text{pl}} \cos\Phi_j) + n_j(X_Q - R_{\text{l}} \tan\Phi_j)\theta. \tag{15}$$

In addition, we accept the following approximation. Let the angles Φ_j satisfy the condition

$$\Phi_j^2 \ll 1, \tag{16}$$

which is equivalent to the following requirement:

$$\left[\frac{Nb_{\text{in}}}{2R_{\text{in}}}\right]^2 \ll 1 \tag{17}$$

(note that condition (16) is appreciably less strict than the requirement $|\Phi_j| \ll 1$). Then, rejecting terms of the order of Φ_j^3 and higher in (15), we obtain

$$\begin{aligned}\delta H_j &= [h(n_x - n_{\text{pl}}) + \theta n_x X_Q] - \theta n_x R_{\text{l}} \Phi_j \\ &+ \frac{n_{\text{pl}}}{2n_x}[h(n_x - n_{\text{pl}}) - \theta n_{\text{pl}} X_Q]\Phi_j^2.\end{aligned} \tag{18}$$

It is seen that the choice of the value $X_Q = 0$ substantially simplifies further analysis. It is this case that we consider below. Thus, formula (18) takes the form

$$\delta H_j = h(n_x - n_{\text{pl}}) - \theta n_x R_{\text{l}} \Phi_j + \frac{n_{\text{pl}}}{2n_x} h(n_x - n_{\text{pl}})\Phi_j^2. \tag{19}$$

The term in (19) that is proportional to Φ_j causes a shift of the spectral characteristic along the frequency scale (see below), and the term proportional to Φ_j^2 distorts its shape. Therefore, we investigate the conditions under which the last term in (19) can be ignored. That is, we require that the following inequality be fulfilled:

$$\frac{n_{\text{pl}}}{2n_x} h|n_x - n_{\text{pl}}|\Phi_j^2 \ll |\theta n_x R_{\text{l}} \Phi_j|. \tag{20}$$

By substituting into it the maximum value $|\Phi_j| \approx Nb_{\text{in}}/2R_{\text{in}}$, we obtain the requirement on the working range of rotation angles

$$|\theta| \gg \frac{n_{\text{pl}}|n_x - n_{\text{pl}}|}{n_x^2} \frac{Nhb_{\text{in}}}{4R_{\text{l}}R_{\text{in}}}. \tag{21}$$

Under these assumptions, formula (19) is simplified and reduced to the relation

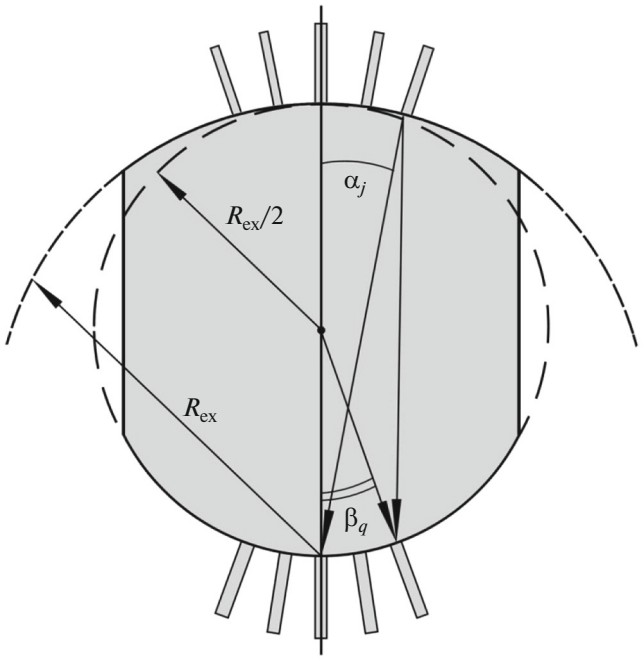

Fig. 3. Output planar waveguide in the Rowland circle geometry [20].

$$\begin{aligned}\delta H_j &= h(n_x - n_{\text{pl}}) - \theta n_x R_{\text{l}} \Phi_j \\ &= h(n_x - n_{\text{pl}}) - \theta n_x \frac{R_{\text{l}}}{R_{\text{in}}} b_{in} j \\ &= h(n_x - n_{\text{pl}}) - \theta b_{\text{ef}} j,\end{aligned} \tag{22}$$

where the following notation is introduced:

$$b_{\text{ef}} \equiv n_x \frac{R_{\text{l}}}{R_{\text{in}}} b_{\text{in}}. \tag{23}$$

4. SPECTRAL CHARACTERISTIC OF THE DEMULTIPLEXER

Transmittance of the demultiplexer at the optical frequency ν (its spectral characteristic) is defined by addition of $N = (2M + 1)$ waves and is given by the relation (q is the number of the receiving waveguide at the output)

$$A_q(\nu) = \left|\sum_{j=-M}^{M} \Gamma_j \exp\left(\frac{2\pi\nu}{c} H_{jq}\right)\right|^2, \tag{24}$$

where the coefficient Γ_j describes the loss in the jth channel waveguide, and c is the speed of light in vacuum. Further we consider a case of uniform power distribution in channels, i.e., we assume that all $\Gamma_j = \Gamma$. For a demultiplexer without a cut, substitution of (5) into (24) using (6) and (7) leads to a well-known result

$$A_q(\nu) = \Gamma^2 \left[\frac{\sin(2M\psi_q)}{\sin\psi_q}\right]^2, \tag{25}$$

where the notation

$$\psi_q \equiv \frac{\pi}{c}(\Delta H)_q \nu \tag{26}$$

is introduced.

It is evident from (25) that $A_q(\nu)$ is a periodic function having sharp transmission peaks at the frequencies

$$\nu_{qm}^{(0)} = \frac{mc}{(\Delta H)_q}, \tag{27}$$

where m are integers (order of interference).

According to (9) and (22), a cut ($h \neq 0$) and a rotation ($\theta \neq 0$) of a part of the input planar waveguide will cause a change in the optical length of the channels

$$\begin{aligned} H_{jq} &= H_{0q}^{(0)} + (\Delta H)_q j + h(n_x - n_{\text{pl}}) - \theta b_{\text{ef}} j \\ &= H_{0q}^{(0)} + h(n_x - n_{\text{pl}}) + \left[(\Delta H)_q - \theta b_{\text{ef}}\right] j. \end{aligned} \tag{28}$$

Substituting (28) into (24) and calculating the sum, we obtain an analogue of formula (25)

$$A_q(\nu) = \Gamma^2 \left[\frac{\sin\left(2M\psi_q(\theta)\right)}{\sin\psi_q(\theta)}\right]^2. \tag{29}$$

But instead of (26) we now have a new definition

$$\psi_q(\theta) \equiv \frac{\pi}{c}\left[(\Delta H)_q - b_{\text{ef}}\theta\right]\nu. \tag{30}$$

The last two relations clearly show that interference resulted in a shift of the spectral characteristic along the frequency scale. A new position of the transmission peaks is easily obtained from these equations

$$\nu_{qm} = \nu_{qm}^{(0)}\left[1 + \frac{b_{\text{ef}}}{(\Delta H)_q}\theta\right]. \tag{31}$$

5. CONDITION FOR THERMAL COMPENSATION OF THE SPECTRAL CHARACTERISTIC

Obviously, when the temperature T varies, the quantities involved in relation (31) will also vary. Let us assume that the external compensating action also changes the cut angle θ

$$\theta = \theta_{\text{com}}(T) \tag{32}$$

and try to find conditions that allow the position of the transmission frequency peaks (31) to be kept unchanged using the above compensation, i.e., we require fulfillment of the condition

$$\frac{\partial}{\partial T}\nu_{qm}(T) = \frac{\partial}{\partial T}\left\{\nu_{qm}^{(0)}\left[1 + \frac{b_{\text{ef}}}{(\Delta H)_q}\theta_{\text{com}}(T)\right]\right\} = 0. \tag{33}$$

It is known that for the initial (i.e., at $h = 0$, $\theta = 0$) demultiplexer the relative frequency peak shift is defined by the relation that can be obtained from (27)

$$\frac{1}{\nu_{qm}^{(0)}}\frac{\partial}{\partial T}\nu_{qm}^{(0)}(T) = -\frac{n_{\text{ch}}}{n_{\text{ch}}^{\text{g}}}\left[\gamma_{\text{ch}} + \frac{1}{n_{\text{ch}}}\frac{\partial n_{\text{ch}}}{\partial T}\right], \tag{34}$$

where γ_{ch} is the coefficient of thermal expansion of the channel wave guide, and n_{ch}^{g} is the group waveguide refractive index of the channel.

After calculating the derivative (33) and rejecting negligibly small quantities, one gets the requirement on the angle of compensation

$$\frac{\partial}{\partial T}\theta_{\text{com}} = \frac{(\Delta H)_q}{b_{\text{ef}}}\frac{n_{\text{ch}}}{n_{\text{ch}}^{\text{g}}}\left[\gamma_{\text{ch}} + \frac{1}{n_{\text{ch}}}\frac{\partial n_{\text{ch}}}{\partial T}\right]. \tag{35}$$

Substituting into it relation (23) for b_{ef} and assuming that, according to (7), $(\Delta H)_q \cong n_{\text{ch}}\Delta L$, we obtain the final result

$$\begin{aligned} \frac{\partial\theta_{\text{com}}}{\partial T} &= \frac{n_{\text{ch}}\Delta L R_{\text{in}}}{n_x b_{\text{in}} R_{\text{l}}}\frac{n_{\text{ch}}}{n_{\text{ch}}^{\text{g}}}\left[\gamma_{\text{ch}} + \frac{1}{n_{\text{ch}}}\frac{\partial n_{\text{ch}}}{\partial T}\right] \\ &= \chi\left[\gamma_{\text{ch}} + \frac{1}{n_{ch}}\frac{\partial n_{\text{ch}}}{\partial T}\right], \end{aligned} \tag{36}$$

where the following dimensionless factor is introduced:

$$\chi \equiv \frac{n_{\text{ch}}^2\Delta L R_{\text{in}}}{n_x n_{\text{ch}}^{\text{g}} b_{\text{in}} R_{\text{l}}}. \tag{37}$$

Using (34), we can write (36) as

$$\frac{\partial\theta_{\text{com}}}{\partial T} = -\chi\frac{1}{\nu_{qm}^{(0)}}\frac{\partial}{\partial T}\left[\nu_{qm}^{(0)}(T)\right]. \tag{38}$$

Thus, the desired derivative of the angle of compensation with respect to temperature is defined by the relative rate of variation with temperature of the peak maximum of the initial demultiplexer multiplied by the geometric factor (37).

5. NUMERICAL ESTIMATES

Let us illustrate estimation of the above results using the values from Table 1. The characteristics of the materials in this table are taken from [21, 22].

The calculated spectral characteristic for these parameter values is shown in Fig. 4.

We check condition (14) that should be fulfilled to ensure applicability of subsequent calculations. Considering definition (12), it reduces to the following requirement:

$$\theta \leq \frac{2R_{\text{in}}h}{NR_{\text{l}}b_{\text{in}}} = \frac{2\times 6.0\times 0.040}{129\times 4.4\times 0.015} \approx 0.056 \text{ rad}, \tag{39}$$

which is easily fulfilled in the working range of angles θ.

Now we estimate the factor χ entering into (36) and defined by (37). An example of the refractive index of the medium filling the cut will the value $n_x = 1.4$. Then the factor χ takes the form

Table 1. Technical and physical AWG parameters used for numerical estimations

Parameter	Symbol	Numerical value
Number of channel waveguides	N	129
Central channel frequency (one of ITU-T standard values)	$\nu_c = \nu_{qm}^{(0)}$	193.80 THz ($\lambda_c = 1546.92$ nm)
Order of interference	m_c	29
Difference of lengths of neighboring channel waveguides	ΔL	30.6 μm
Radius of channel arrangement at input	R_{in}	6.0 mm
Radius of channel arrangement at output	R_{ex}	6.0 mm
Period of channel arrangement at input	b_{in}	15 μm
Period of channel arrangement at output	b_{ex}	15 μm
Distance from point of radiation injection in AWG to line of planar waveguide cut	R_1	4.4 mm
Width of cut in input planar waveguide	h	40 μm
Effective refractive index of channel waveguide at 20°C	n_{ch}	1.455
Group effective refractive index of channel waveguide at 20°C	n_{ch}^g	1.473
Effective refractive index of planar waveguide at 20°C	n_{pl}	1.450
Thermal expansion coefficient of channel waveguide	γ_{ch}	4×10^{-6} K^{-1}
Derivative of effective refractive index of channel waveguide with respect to temperature	$\frac{\partial n_{ch}}{\partial T}$	1.0×10^{-5} K^{-1}

$$\chi = \frac{n_{ch}^2 \Delta L R_{in}}{n_x n_{ch}^g b_{in} R_1} = \frac{1.455^2 \times 30.6 \times 6.0}{1.4 \times 1.473 \times 15 \times 4.4} \approx 3.24 \quad (40)$$

and correspondingly

$$\frac{\partial \theta_{com}}{\partial T} = 3.24\left[4 \times 10^{-6} + \frac{1}{1.455} 1.0 \times 10^{-5}\right] \approx 3.5 \times 10^{-5} \text{ rad/K}. \quad (41)$$

Note that formula (38) is more suitable for practical application than (36), because the relative frequency shift (34) can be measured before interreference in the demultiplexer, and this experiment is simpler than measurements of several quantities entering into (36). When choosing the medium to fill the gap, one should also remember that the condition $n_x \approx n_{pl} \approx n_{ch}$ should be followed to minimize the Fresnel reflection loss in the cut. A similar choice also makes it easier to fulfil requirement (21) that the rotation angles of the entire working range should satisfy. In our example it means that

$$|\theta| \ll \frac{1.45 \times 0.05 \times 129 \times 0.040 \times 0.015}{1.4^2 \times 4 \times 4.4 \times 6.0} \approx 2.7 \times 10^{-5} \text{ rad}. \quad (42)$$

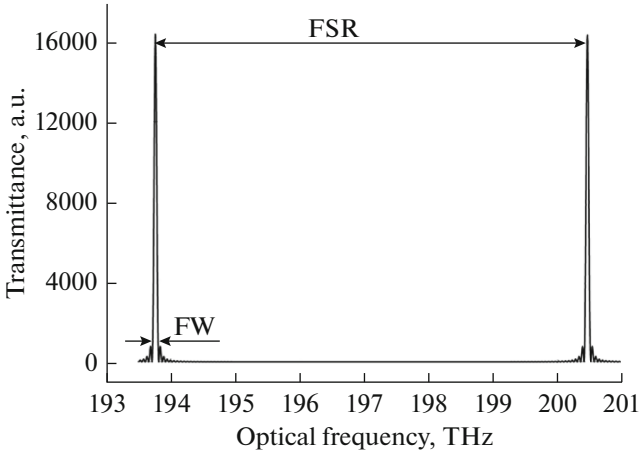

Fig. 4. Example of the spectral characteristic of the arrayed waveguide grating. The channel transmission band is (FW) ≈ 100 GHz; the free spectral region is (FSR) ≈ 6.4THz.

It should be noted that, according to (31), the choice of a nonzero initial (i.e., at room temperature) angle θ_0 will actually shift the transmission peak frequency, which should be taken into account in developing the demultiplexer.

6. CONCLUSIONS

A method for passive thermal compensation of an AWG demultiplexer using a cut in the input planar waveguide and controllable rotation of a part of this waveguide has been investigated. A possibility of implementing this thermal compensation is shown, restrictions on the choice of demultiplexer parameters to be observed for demultiplexer functioning are obtained, and the corresponding recommendations are given. A simple analytical expression for the deriv-

ative of the compensation angle with respect to temperature is obtained, which is needed for the development of the multiplexer. In the given numerical example, this derivative is 3.5×10^{-5} rad/K.

APPENDIX

The optical path length H_{jq} of the wave propagating through the channel waveguide with number j and arriving at the output receiving waveguide with number q is composed of several terms. In Fig. 2, it is seen that

$$\begin{aligned} H_{jq} &= n_{\text{pl}}\left|ED_j\right| + n_x\left|D_jA_j\right| \\ &+ n_{\text{pl}}\left|A_jT_j\right| + n_{\text{ch}}L_j + n_{\text{pl}}R_{\text{ex}}f_{jq}, \end{aligned} \tag{A1}$$

where $|ED_j|$, $|D_jA_j|$, and $|A_jT_j|$ are the lengths of the corresponding segments.

The use of refraction laws at the boundaries of the cut and an assumption that perturbation of refraction angles caused by the cut ($h \neq 0$) and the rotation ($\theta \neq 0$) is small lead (after rather cumbersome calculations) to the following results:

$$\begin{aligned} \left|ED_j\right| + \left|A_jT_j\right| &= R_{\text{in}} - \left(\cos\Phi_j + \frac{n_{\text{pl}}}{n_j}\sin^2\Phi_j\right)h \\ &- \theta\left(X_Q - R_{\text{l}}\tan\Phi_j\right)\frac{n_{\text{pl}}}{n_j}\sin^2\Phi_j, \end{aligned} \tag{A2}$$

$$\left|D_jA_j\right| = \frac{n_x}{n_j}\left|h + (X_Q - R_{\text{l}}\tan\Phi_j)\theta\right|, \tag{A3}$$

where

$$n_j \equiv \sqrt{n_x^2 - n_{\text{pl}}^2\sin^2\Phi_j}. \tag{A4}$$

After substitution of (A2) and (A3) into (A1) and some simple transformations we get

$$\begin{aligned} H_{jq} &= n_{\text{pl}}\left[R_{\text{in}} - h\cos\Phi_j\right] + n_jh_j(\theta) \\ &+ \frac{n_x^2}{n_j}\left[\left|h_j(\theta)\right| - h_j(\theta)\right] + n_{\text{ch}}L_j + n_{\text{pl}}R_{\text{ex}}f_{jq}, \end{aligned} \tag{A5}$$

where

$$h_j \equiv h + \left(X_Q - R_{\text{l}}\tan\Phi_j\right)\theta. \tag{A6}$$

FUNDING

The work was supported by the Zelenograd Nanotechnological Center (ZNTC Co.). All rights to the usage of the results belong to the ZNTC Co.

CONFLICT OF INTEREST

The authors declare that they have no conflicts of interest.

REFERENCES

1. V. R. Marrazzo, F. Fienga, M. Riccio, A. Irace, and G. Breglio, "Multichannel approach for arrayed waveguide grating based FBG interrogation systems," *Sensors* **21** (18), 6214 (2021). https://doi.org/10.3390/s21186214
2. H. Li, Y. Li, E. Li, X. Dong, Y. Bai, Y. Liu, and W. Zhou, "Temperature-insensitive arrayed waveguide grating demodulation technique for fiber Bragg grating sensor," *Opt. Laser Technol.* **51**, 77–81 (2013). https://doi.org/10.1016/j.optlastec.2013.04.002
3. Y. C. Xu, Q. N. Wang, and W. Z. Zhu, "Design and simulation of arrayed waveguide grating for miniature Raman spectrometer," *Appl. Mech. Mater.* 644–650, 3588–3592 (2014). https://doi.org/10.4028/www.scientific.net/AMM.644-650.3588
4. P. Muñoz, R. García-Olcina, J. D. Doménech, M. Rius, J. Capmany, L. Chen, C. Habib, X. J. M. Leijtens, T. de Vries, M. J. R. Heck, L. Augustin, R. Nötzel, and D. Robbins, "Multi-wavelength laser based on an Arrayed Waveguide Grating and Sagnac loop reflectors monolithically integrated on InP," *Proc. 15th Eur. Conf. on Integrated Optics (ECIO 2010), Cambridge, UK, April 7–9, 2010* (IEEE, 2010), pp. 1–2. https://www.ecio-conference.org/wp-content/uploads/2016/05/2010/ECIO-2010_WeF2.pdf
5. A. Stoll, Z. Zhang, R. Haynes, and M. Roth, "High-resolution arrayed-waveguide-gratings in astronomy: Design and fabrication challenges," *Photonics* **4** (2), 30 (2017). https://doi.org/10.3390/photonics4020030
6. M. Yasumoto, T. Suzuki, A. Tate, and H. Tsuda, "Arrayed-waveguide grating with wavefront compensation lenses for spatial filter integration," *IEICE Electron. Express* **3** (11), 221–226 (2006). https://doi.org/10.1587/elex.3.221
7. *Ultrafast Lasers: Technology and Applications*, Ed. by M. E. Fermann, A. Galvanauskas, and G. Sucha (Marcel Dekker, New York, 2003).
8. J. Meyer, A. Nedjalkov, E. Pichler, C. Kelb, and W. Schade, "Development of a polymeric arrayed waveguide grating interrogator for fast and precise lithium-ion battery status monitoring," *Batteries* **5** (4), 66 (2019). https://doi.org/10.3390/batteries5040066
9. H. Ehlers, M. Biletzke, B. Kuhlow, G. Przyrembel, and U. H. P. Fischer, "Optoelectronic packaging of arrayed-waveguide grating modules and their environmental stability tests," *Opt. Fiber Technol.* **6** (4), 344–356 (2000). https://doi.org/10.1006/ofte.2000.0341
10. D.-L. Li, C.-S. Ma, Z.-K. Qin, H.-M. Zhang, D.-M. Zhang, and S.-Y. Liu, "Design of athermal arrayed waveguide grating using silica/polymer hybrid materials," *Opt. Appl.* **37** (3), 305–312 (2007). https://dbc.wroc.pl/Content/63129/optappl_3703p305.pdf
11. K. Maru, Y. Abe, M. Ito, H. Ishikawa, S. Himi, H. Uetsuka, and T. Mizumoto, "2.5%-Δ silica-based athermal arrayed waveguide grating employing spot-size converters based on segmented core," *IEEE Photonics Technol.*

Lett. **17** (11), 2325–2327 (2005). https://doi.org/10.1109/LPT.2005.857233

12. K. Maru and Y. Abe, "Low-loss, flat-passband and athermal arrayed waveguide grating multi/demultiplexer," *Opt. Express* **15** (26), 18351–18356 (2007) https://doi.org/10.1364/OE.15.018351
13. A. Kaneko, S. Kamei, Y. Inoue, H. Takahashi, and A. Sugita, "Athermal silica-based arrayed-waveguide grating (AWG) multiplexers with new low loss groove design," *Proc. Optical Fiber Communication Conf. and the Int. Conf. on Integrated Optics and Optical Fiber Communication, San Diego, CA, USA, February 21–26, 1999* (IEEE, 1999), pp. 204–206. https://doi.org/10.1109/OFC.1999.767839
14. S. Kamei, Y. Inoue, T. Shibata, and A. Kaneko, "Low-loss and compact silica-based athermal arrayed waveguide grating using resin-filled groove," *J. Lightwave Technol*. **27** (17), 3790–3799 (2009). https://doi.org/10.1109/JLT.2008.2007657
15. S. Kamei, K. Iemura, A. Kaneko, Y. Inoue, T. Shibata, H. Takahashi, and A. Sugita, "1.5%-Δ athermal arrayed-waveguide grating multi/demultiplexer with very low loss groove design," *IEEE Photonics Technol. Lett*. **17** (3), 588–590 (2005). https://doi.org/10.1109/LPT.2004.840990
16. T. Zhou and W. Ma, "A novel fabrication approach for an athermal arrayed-waveguide grating," *J. Semicond*. **31** (1), 014005 (2010). https://doi.org/10.1088/1674-4926/31/1/014005
17. J. Hasegawa and K. Nara, "Ultra-wide temperature range (−30~70°C) operation of athermal AWG module using pure aluminum plate," *Proc. Optical Fiber Communication Conf. and Exposition and the National Fiber Optic Engineers Conf., Anaheim, California, March 5–10, 2006* (Opt. Publ. Group, 2006), p. OWI68.
18. B. P. Mcginnis, US Patent No. 8,538,212 B2 (2011).
19. R. Cole, M. Guerrero, K. Purchase, A. J. Ticknor, K. Mcgreer, D. Menche, and P. D. Ascanio, EP Patent No. 1,743,201 B1 (2004).
20. R. Marz, *Integrated Optics: Design and Modeling* (Artech House, Norwood, MA, 1994).
21. *Encyclopedic Handbook of Integrated Optics*, Ed. by K. Iga and Y. Kokubun (CRC Press, Boca Raton, 2006). https://doi.org/10.1201/9781315220949
22. T. Saito, K. Nara, K. Tanaka, Y. Nekado, J. Hasegawa, and K. Kashihara, "Temperature-insensitive (athermal) AWG modules," *Furukawa Rev*. **24**, 29–33 (2003).

Translated by M. Potapov